Electronic Supplementary Material (ESI) for ChemComm.

Supporting Information

A luminescent heptanuclear Ir_6Dy complex showing field-induced slow magnetization relaxation

Dai Zeng, Min Ren, Song-Song Bao, Li Li and Li-Min Zheng*

Experimental Section

All chemicals and solvents were of reagent grade and used as purchased. The 2-pyridylphosphonic acid ($2\text{-}C_5H_4NPO_3H_2$, 2-bppH_2) was prepared according to the literature procedure.[1] $[Ir(ppy)_2(\mu\text{-}Cl)]_2$ was synthesized according to the Noyama route by refluxing $IrCl_3 \cdot 3H_2O$ with 2.2 equiv of 2-phenylpyridine (ppy) in a 3:1 mixture of 2-ethoxyethanol and water.[2] The microwave-assisted reactions were conducted using a Biotage Initiator^{TM} EXP instrument. Elemental analyses for C, H and N were determined with a Perkin Elmer 240C elemental analyzer. Infrared spectra were measured as KBr pellets on a Bruker Tensor 27 spectrometer in the range of 400-4000 cm^{-1}. Thermogravimetric analysis (TGA) were performed on a Mettler-Toledo TGA/DSC STARe thermal analyzer in the range of 25-800°C under a nitrogen flow at a heating rate of 5ºC/min. Powder X-ray diffraction (PXRD) data were recorded on a Bruker D8 ADVANCE X-ray powder diffractometer (Cu-Kα) over the 2θ range of 5 to 50° at room temperature. The UV-vis and luminescence spectra were recorded on Perkin Elmer Lambda 950 UV/Vis/NIR Spectrometer and Perkin Elmer LS55 fluorescence spectrometer at room temperature, respectively. The magnetic susceptibility data were recorded on a Quantum Design MPMS-XL7 SQUID magnetometer and a Quantum Design MPMS SQUID VSM system. The diamagnetic contribution of the sample itself was estimated from Pascal's constant.[3]

Synthesis of $[Ir(ppy)_2(bppH)]$: 2-Pyridylphosphonic acid (bppH_2) (2.2 mmol, 0.3564g) was dissolved in 10 cm^3 CH_2Cl_2 in the presence of triethylamine (3.6 mmol, 0.3656g) and then added to a CH_2Cl_2 solution (200 cm^3) of $[Ir(ppy)_2Cl]_2$ (1 mmol, 1.072g). The above solution was stirred for one day at room temperature, resulting in the formation of a yellow precipitate. The precipitate was collected by suction filtration, washed with a minimum amount of water and CH_2Cl_2. Yield: 76%. ESI-MS: m/z: 658 [M^-]. Elemental analysis calcd for $C_{27}H_{21}N_3O_3PIr$: C, 49.23; H, 3.21; N, 6.38%. Found: C, 48.87; H, 3.68; N, 6.14%. IR (KBr, cm^{-1}): 3423(s), 3057(w), 1605(s), 1581(s), 1560(w), 1478(s), 1437(m), 1420(s), 1306(w), 1268(m), 1225(w), 1159(s), 1086(m), 1061(m), 1030(m), 920(m), 757(s), 729(s), 669(w), 629(w), 582(m), 524(w), 455(w), 420(w).

Synthesis of compound 1. $Dy(CF_3SO_3)_3$ (0.0122g, 0.02 mmol) was added to a methanol solution (5 cm^3) of [$Ir(ppy)_2(bppH)$] (0.0135 g, 0.02 mmol). After heating the yellow solution at 100 ℃ under microwave irradiation for 30 min, the filtrate was left to stand for one week at room temperature. Yellow block crystals were collected by suction filtration, washed with a minimum amount of methanol. Yield: 41%. Elemental analysis calcd for $C_{162}H_{124}N_{18}O_{18}P_6DyIr_6\cdot CF_3SO_3\cdot 8H_2O$: C, 44.43; H, 3.20; N, 5.72%. Found: C, 43.68; H, 3.69; N, 5.34%. IR (KBr, cm^{-1}): 3427(s), 3059(w), 1634(w), 1607(m), 1583(m), 1562(w), 1479(s), 1422(m), 1267(m), 1225(w), 1159(s), 1122(s), 1063(m), 1032(m), 973(w), 931(w), 758(s), 730(s), 669(w), 639(w), 583(m), 520(w), 442(w), 420(w).

Single-Crystal Structure Determination. A single crystal of dimensions 0.20 × 0.20 × 0.05 mm^3 for compound **1** was mounted on a glass rod. The crystal data were collected on a Bruker SMART APEX DUO diffractometer using monochromated Mo-Kα radiation (λ = 0.71073 Å) at 123 K for **1**. The structures were solved by direct methods and refined on F^2 by full matrix least squares using SHELXTL. All non-hydrogen atoms were refined anisotropically. All hydrogen atoms were either put in calculated positions or found from the difference Fourier maps and refined isotropically. Selected bond lengths and angles are given in Table S1.

References

1. J. S. Loran, R. A. Naylor and A. Williams, *Journal of the Chemical Society, Perkin Transactions 2,* 1976, **12**, 1444-1447.
2. M. Nonoyama, *Bulletin of the Chemical Society of Japan*, 1974, **47**, 767-768.
3. O. Kahn, *Molecular Magnetism*, VCH Publishers, Inc., New York, **1993**.

Table S1. Selected bond lengths (Å) and angles (deg) for compound **1**[a].

Dy(1)-O(1)	2.253(8)	Ir(2)-N(4)	2.164(7)
Dy(1)-O(4)	2.220(8)	Ir(2)-N(5)	2.046(10)
Dy(1)-O(7)	2.223(9)	Ir(2)-N(6)	2.127(7)
Ir(1)-C(16)	2.016(9)	Ir(2)-O(5)	2.186(7)
Ir(1)-C(27)	1.997(10)	Ir(3)-C(70)	1.949(17)
Ir(1)-N(1)	2.156(9)	Ir(3)-C(81)	1.941(15)
Ir(1)-N(2)	2.047(10)	Ir(3)-N(7)	2.194(12)
Ir(1)-N(3)	2.027(9)	Ir(3)-N(8)	1.911(8)
Ir(1)-O(2)	2.203(7)	Ir(3)-N(9)	2.013(8)
Ir(2)-C(43)	1.982(12)	Ir(3)-O(8)	2.177(9)
Ir(2)-C(54)	1.992 (13)		
O(1)-Dy(1)-O(4)	92.9(3)	C(43)-Ir(2)-N(5)	81.4(4)
O(4)-Dy(1)-O(7)	90.1 (3)	O(5)-Ir(2)-N(4)	82.0(3)
O(1)-Dy(1)-O(7)	88.2(3)	C(54)-Ir(2)-N(6)	79.6(4)
O(2)-Ir(1)-N(1)	81.6(3)	C(70)-Ir(3)-N(8)	81.8(5)
C(16)-Ir(1)-N(2)	81.1(4)	C(81)-Ir(3)-N(9)	81.6(5)
C(27)-Ir(1)-N(3)	80.7(4)	O(8)-Ir(3)-N(7)	82.1(4)

Table S2. Hydrogen bond lengths (Å) and angles (deg) for compound **1**[a].

D-H···A	*d*(D-H)	*d*(H···A)	*d*(D···A)	∠ DHA
O3A-H3a···O6	0.8400	1.6500	2.432(12)	153.00
O9-H9c···O1WB	0.8500	1.7300	2.506(16)	150.00
O1WB-H1WdB···O3WB	0.8500	1.9300	2.77(2)	172.00
O1WB-H2WdB···O5A	0.8500	1.9100	2.695(15)	153.00
O2WB-H2WcB···O6A	0.8500	2.0200	2.72(2)	139.00
O4W-H4Wd···O11	0.8500	2.0700	2.63(3)	123.00
O4W-H4Wb···O11C	0.8500	1.9400	2.60(3)	133.00

[a] Symmetry codes: (A) -x, -y+2, -z; (B) –x+1, -y+1, -z; (C) –x+1, -y+1, -z+1.

Table S3. Lanthanide geometry analysis by SHAPE software.

CShM	**1**
octahedron (O_h)	0.03821
trigonal prism (D_{3h})	16.33390

Table S4. The parameters obtained by fitting the χ_M'' versus frequency data for compound **1** in different *dc* fields at 2 K.

H / kOe	χ_T / cm^3·mol^{-1}	χ_S / cm^3·mol^{-1}	ln(τ / s)	α	R^a
0.5	6.48	0.77	-6.95	0.383	1.8×10^{-5}
1.0	6.20	0.40	-6.39	0.431	5.8×10^{-5}
1.5	5.68	0.28	-6.39	0.461	9.7×10^{-5}
2.0	5.02	0.31	-6.62	0.473	1.2×10^{-4}
2.5	4.29	0.42	-6.98	0.456	2.8×10^{-4}
3.0	3.53	0.65	-7.30	0.390	3.4×10^{-4}

$^aR = \sum[(\chi'_{obs} - \chi'_{cal})^2 + (\chi''_{obs} - \chi''_{cal})^2] / \sum[\chi'^2_{obs} + \chi''^2_{obs}]$

Table S5. The parameters obtained by fitting the χ_M'' versus frequency data for compound **1** under 1 kOe *dc* field.

T / K	χ_T / cm^3·mol^{-1}	χ_S / cm^3·mol^{-1}	ln(τ / s)	α	R^a
2.5	5.05	0.63	-6.86	0.437	1.6×10^{-4}
3.0	4.32	0.90	-7.11	0.413	1.1×10^{-4}
3.5	3.69	1.12	-7.40	0.349	8.9×10^{-5}
4.0	3.24	1.19	-7.75	0.303	5.5×10^{-5}
4.5	2.89	1.19	-8.16	0.275	4.1×10^{-5}
5.0	2.60	1.18	-8.60	0.252	4.8×10^{-5}
5.5	2.37	1.07	-9.18	0.271	2.3×10^{-5}
6.0	2.18	0.96	-9.79	0.278	2.5×10^{-5}
6.5	2.03	0.90	-10.44	0.336	3.4×10^{-5}
7.0	1.90	1.00	-11.00	0.420	3.8×10^{-5}
7.5	1.78	1.15	-11.39	0.496	3.9×10^{-5}

$^aR = \sum[(\chi'_{obs} - \chi'_{cal})^2 + (\chi''_{obs} - \chi''_{cal})^2] / \sum[\chi'^2_{obs} + \chi''^2_{obs}]$

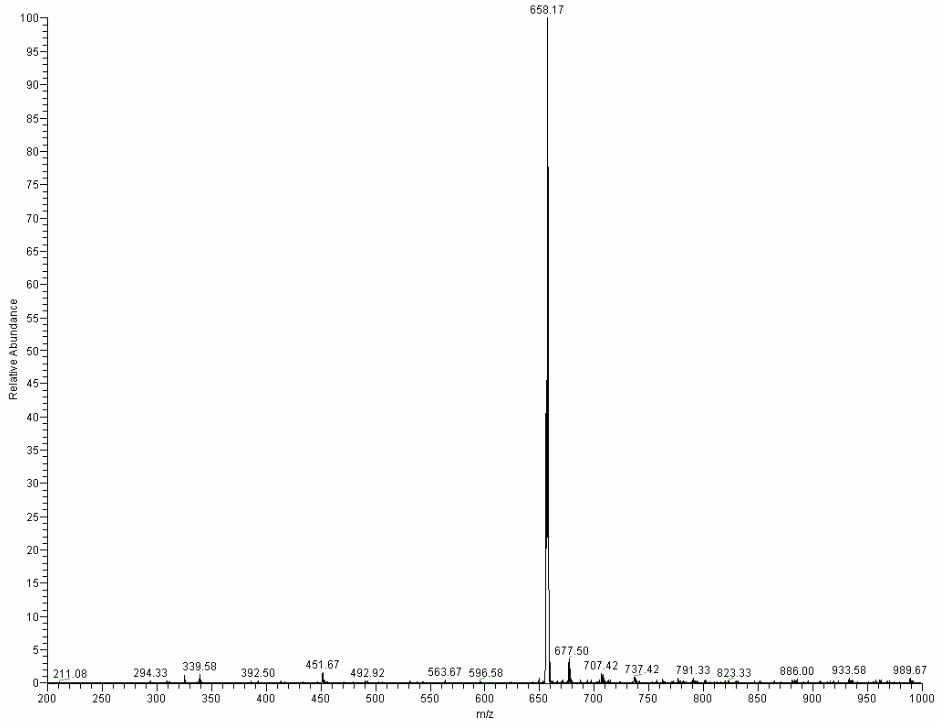

Figure S1. ESI-MS spectra of $[Ir(ppy)_2(bppH)]$ at value of m/z = 658.

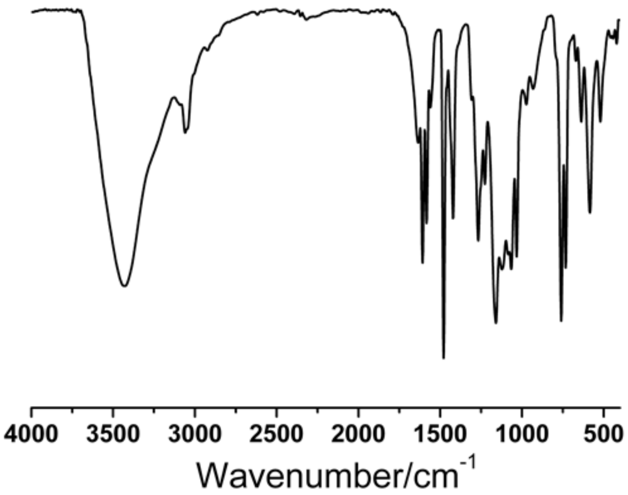

Figure S2. IR spectra for compound **1**

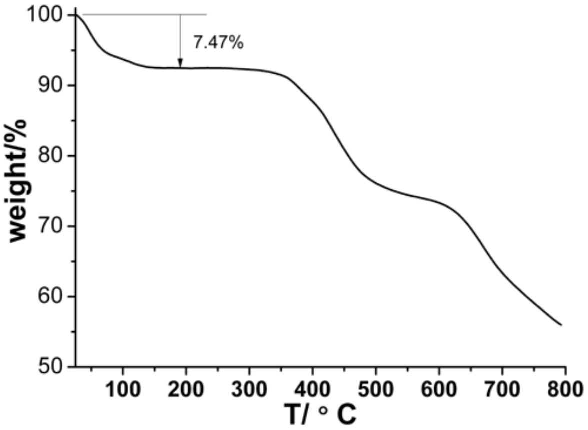

Figure S3. TG curve of **1**. The weight loss of 7.5% in the temperature range of 25 to 150°C is close to the calculated value for the release of eight lattice water molecules and one $CF_3SO_3^-$ anion (6.7%).

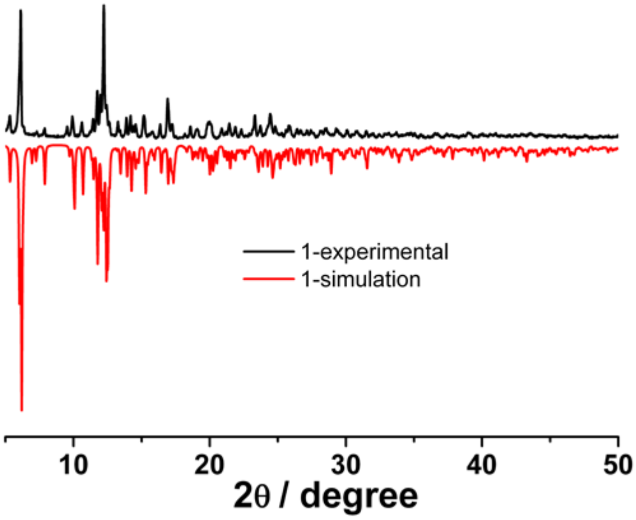

Figure S4. The powder XRD patterns for compound **1**. The pattern simulated from the single crystal data of compound **1** is also given.

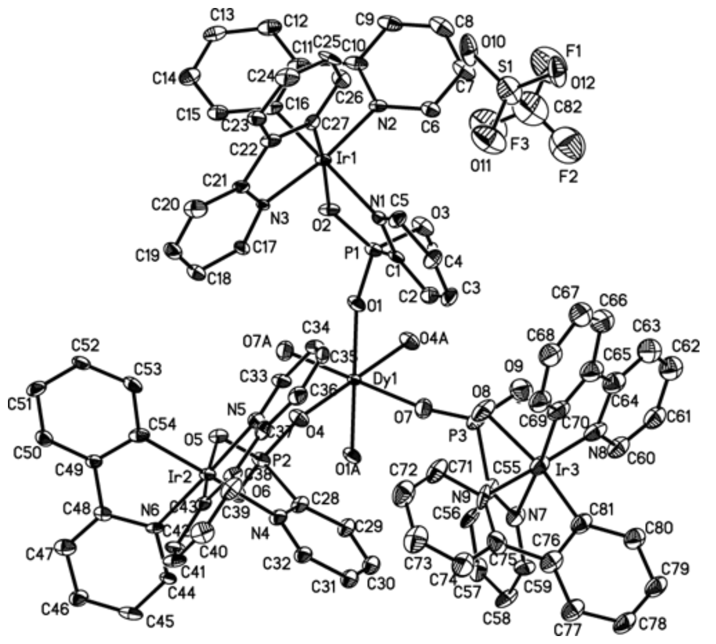

Figure S5. The building unit of **1** in ORTEP view (30% thermal ellipsoids). All lattice water molecules and H atoms except those attached to the phosphonate oxygen atoms are omitted for clarity. Symmetry transformations used to generate equivalent atoms: A: -x, -y+2, -z.

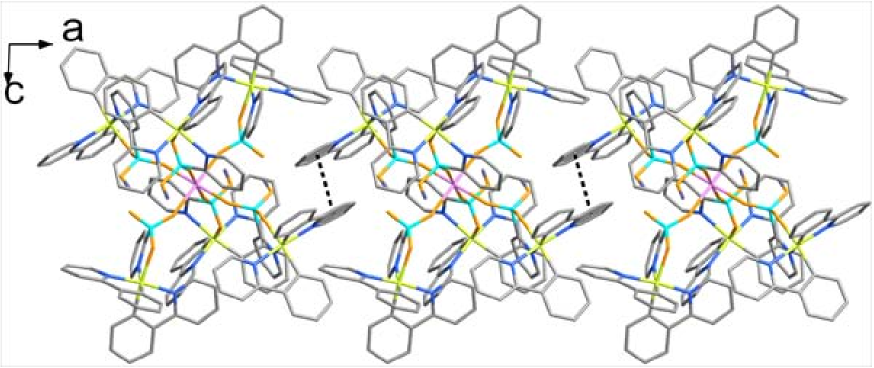

Figure S6. The π-π interactions between two adjacent clusters.

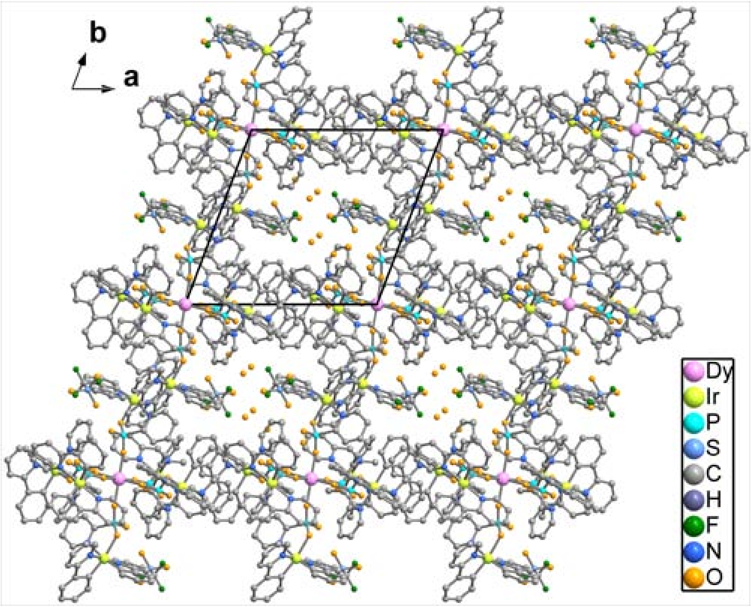

Figure S7. Packing diagram of structure **1** viewed along the *c*-axis.

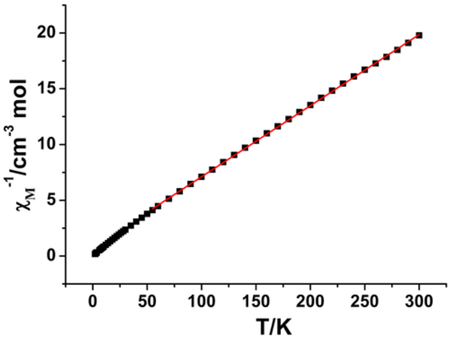

Figure S8. Plots of the $1/\chi_M$ versus T for compound **1**. The red solid line represents the best fit of the data above 50 K.

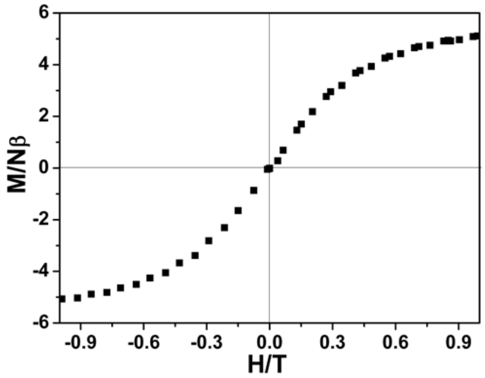

Figure S9. Hysteresis loops in the range of 0-70 kOe for compound **1** at 2 K with sweep rates of 700 Oe/s.

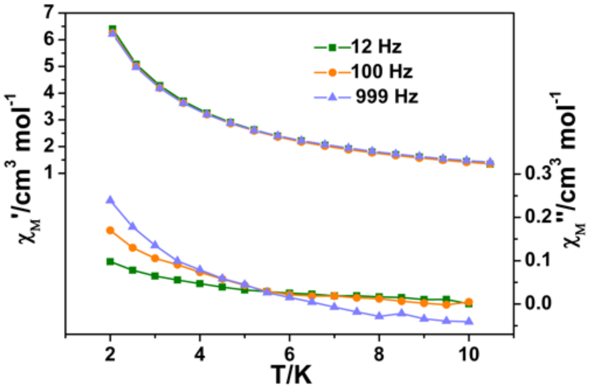

Figure S10. Temperature dependent in-phase (χ_M') and out-of-phase (χ_M'') signals for compound **1** under zero dc field.

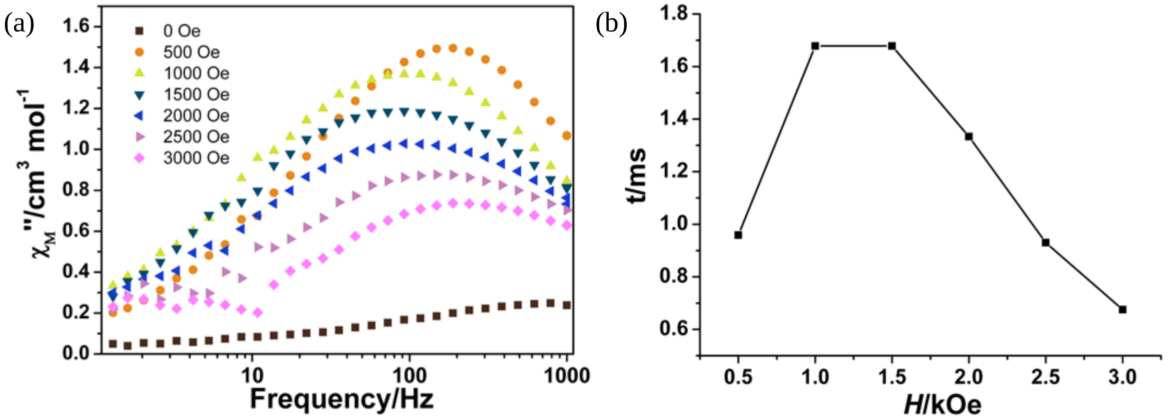

Figure S11. Frequency dependence of the out-of-phase susceptibility (a) and field dependence of the magnetic relaxation time (b) of compound **1** at 2 K under different dc fields.

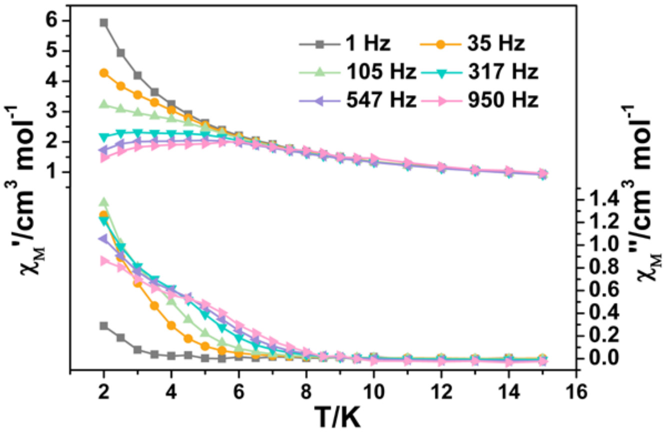

Figure S12. χ_M' and χ_M'' versus temperature plots for compound **1** under 1 kOe dc field.

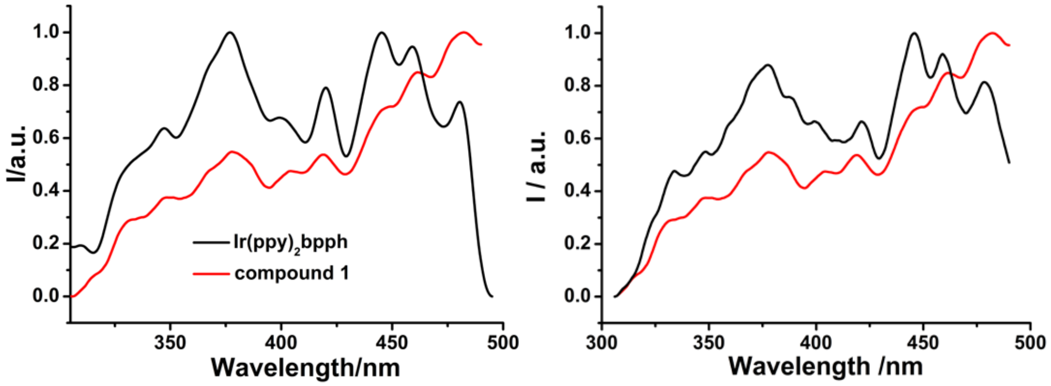

Figure S13. (left) Excitation spectra of compounds **1** and [Ir(ppy)$_2$(bppH)] monitored at 531 nm and 538 nm, respectively; (right) Excitation spectra of compound **1** monitored at 538 nm (red) and 574 nm (black), respectively. 574 nm is characteristic emission of Dy^{III} $^4F_{9/2} \rightarrow {}^6H_{15/2}$.

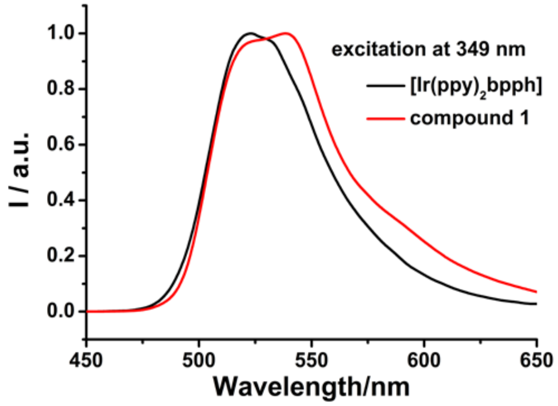

Figure S14. Solid state emission spectrum for compounds **1** and [Ir(ppy)$_2$(bppH)] upon excitation at 349 nm which corresponds to the Dy^{III} $^6H_{15/2} \rightarrow {}^6P_{7/2}$ absorption.

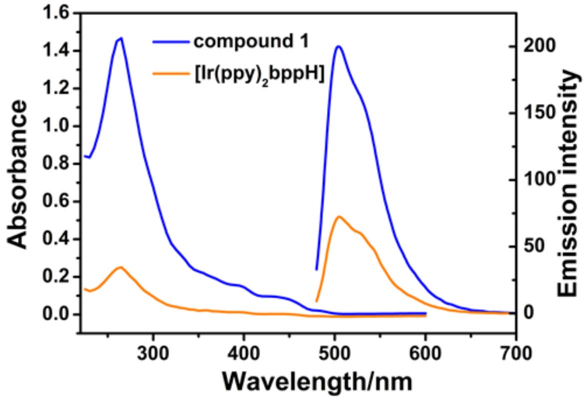

Figure S15. UV-vis absorption spectra and emission spectra for compounds **1** and [Ir(ppy)$_2$(bppH)] in methanol (1×10^{-5} M) under the excitation at 460 nm at room temperature.